Trends in *ortho*-carboranes 1-X-2-R-1,2-$C_2B_{10}H_{10}$ (R = Ph, Me) bearing an *exo*-CN-bonded substituent group (X = NO, N=NR' or NHR'')

Mark A. Fox,[a,*] Richard J. Peace,[a] William Clegg,[b] Mark R.J. Elsegood[b,†] and Kenneth Wade[a,*]

[a] Chemistry Department, Durham University Science Laboratories, South Road, Durham, DH1 3LE, U.K. E-mail: m.a.fox@durham.ac.uk, kenneth.wade@durham.ac.uk

[b] School of Chemistry, Newcastle University, Newcastle upon Tyne, NE1 7RU, U.K.

[†] Current address: Chemistry Department, Loughborough University, Loughborough, Leicestershire, LE11 3TU, U.K.

Abstract

The preparation and crystal structures of four *ortho*-carboranyl-nitrogen compounds, $PhCb^oN{=}N(C_6H_4Me\text{-}4)$ (**1**), $PhCb^oNHNH(C_6H_4Me\text{-}4)$ (**2**), $MeCb^oNHNHPh$ (**3**) and $PhCb^oNHOH$ (**4**) (Cb^o = 1,2-$C_2B_{10}H_{10}$; nitrogen groups at cage carbon C1, Ph or Me at C2), the last as a 1,4-dioxane solvate, are reported. Comparisons of their structures with those of other *ortho*-carboranyl-nitrogen systems studied earlier reveal further correlations between their cage C–C and *exo*-C–N bond distances and bond orders. Substituent orientations and bond distances (cage C1–C2, *exo* C1–N) in RCb^oNHR'' systems (R = Ph or Me at C2) are consistent with dative π-bonding from a nitrogen lone pair into the cage carbon *p*-AO otherwise responsible for cage C1–C2 σ bonding. The N=O and N=NR' residues in RCb^oX prefer to be orientated in plane with the cage C1–C2 in contrast to the RCb^oNHR'' systems. Their C1–C2 bond distances are remarkably sensitive to the planar (sp^2) or pyramidal (sp^3) nature of the NHR" group. Correlations between their cage C–C and *exo*-C–N bond distances and the ^{11}B NMR chemical shifts of their antipodal boron atoms reflect the π-bonding characteristics of the nitrogen substituent.

Introduction

The remarkable capacity of π-donor substituents, attached to carbon atoms of an *ortho*-carborane C_2B_{10} cage, to influence cage C1–C2 bond lengths was first detected some two decades ago [1] with the structural characterisation of the proton sponge salt of the anion $PhCb^oO^-$, (Cb^o = 1,2-$C_2B_{10}H_{10}$; O^- at cage carbon C1, Ph at C2) followed by many related studies [2,3] on *ortho*-carboranes containing thiolato and phosphino groups. However, this area has only recently been documented systematically by experimental and computational studies on systems RCb^oX and XCb^oX in which X is a potential π-donor such as NH_2, OH, SH or anions derived therefrom by deprotonation [4,5]. *Exo*-C=X π-bonding in these systems between the cage carbon atom and substituent X involves a tangentially oriented *p*-AO on carbon that would otherwise be involved in cage bonding, and C1–C2 bond lengthening will occur if the *p*-AO used for *exo* C=X π-bonding is the *p*-AO that in *ortho*-carborane itself is involved in C1–C2 σ-bonding (AO = atomic orbital; Figure 1).

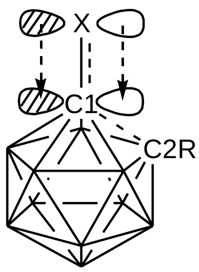

Figure 1. Orbitals involved in the *exo* π-bonding for RCb^oX where X is a π-donating group and R is not a donor group.

The extent to which the cage C1–C2 bond is affected by *exo* π-bonding will therefore depend on the orientation of the substituent in the *exo*-CN systems explored here. Though many *ortho*-carborane derivatives with *exo*-C–N bonds are known, only three structural studies have been carried out elsewhere to our knowledge: the first was on a rhenium complex $^iPrCb^oN_2Re(CO)_4$ [6], which contains a 6-membered –Re–N=N–C–B–H– ring in which the metal atom is attached to one nitrogen atom and to a boron-attached hydrogen; the second was on a hydrazocarborane, HCb^oNRNHR (R = $CO_2{}^tBu$) [7], which contains an intramolecular cage C–H…O hydrogen bond [8]; and the third was on a zirconium complex, $PhN_3Cb^oZrCp_2$ [9], which contains a 3-membered ZrN_2 ring. All three systems thus contain intramolecular interactions that influence the orientation about nitrogen at C1 with respect to the cage C1–C2 bond.

In 2004, we reported the crystal structures of $PhCb^oNH_2$ and the adduct $PhCb^oNH_2{\cdot}OP(NMe_2)_3$ which revealed six independent molecules with C1–C2 bond distances ranging between 1.74 and 1.85 Å [4]. We also reported improved syntheses of *ortho*-carborane nitroso derivatives RCb^oNO and dicarboranylamines $(RCb^o)_2NH$ (R = Ph, Me) and discussed their structures, which in the case of the secondary amines (and amides $[(RCb^o)_2N]^-$ derived therefrom) showed significant cage distortion (C1–C2 bond lengthening) attributable to *exo* C=N π-bonding [10,11]. To supplement these studies, we have carried out a synthetic, spectroscopic, structural and computational investigation of the compounds RCb^oX (R = Ph, Me; X = NNR', NHNHR', NHOH; R' = Ph or C_6H_4Me-4), and further spectroscopic and computational studies on systems with X = NH_2, NO, $NHCb^oR$ and $[NCb^oR]^-$, which have revealed hitherto unremarked characteristics and trends in *ortho*-carborane systems RCb^oX containing *exo* CN units, which we report here.

Results and Discussion

In this section, we outline the synthetic procedures used to prepare the new compounds, and describe their structures. We then explore the structural, bonding and spectroscopic characteristics of *ortho*-carboranyl-nitrogen systems $RCb^oN{=}O$, $RCb^oN{=}NR'$ and RCb^oNHR'' in general, including both the new systems and those previously characterised [4,10]. We also compare the structural and bonding relationships of these 3D pseudoaromatic cages with 2D aromatic ring analogues.

Synthetic Aspects

Scheme 1 summarises the experimental procedures used for the syntheses of the carboranes investigated in this definitive study. Synthetic methods that have not been reported in our earlier papers [4,10] are described in detail in the Experimental section. The azocarboranes were synthesised using a reported literature procedure [12]. The reductions of the nitroso-carboranes RCb^oNO with hydrogen using a palladium/carbon catalyst gave the known [13,14] hydroxylamines RCb^oNHOH in high yields. High-yield reductions of the azocarboranes $RCb^{o}NNAr$ to the hydrazines $RCb^{o}NHNHAr$ were carried out here using the reducing agents, $LiAlH_4$ and Zn/HCl.

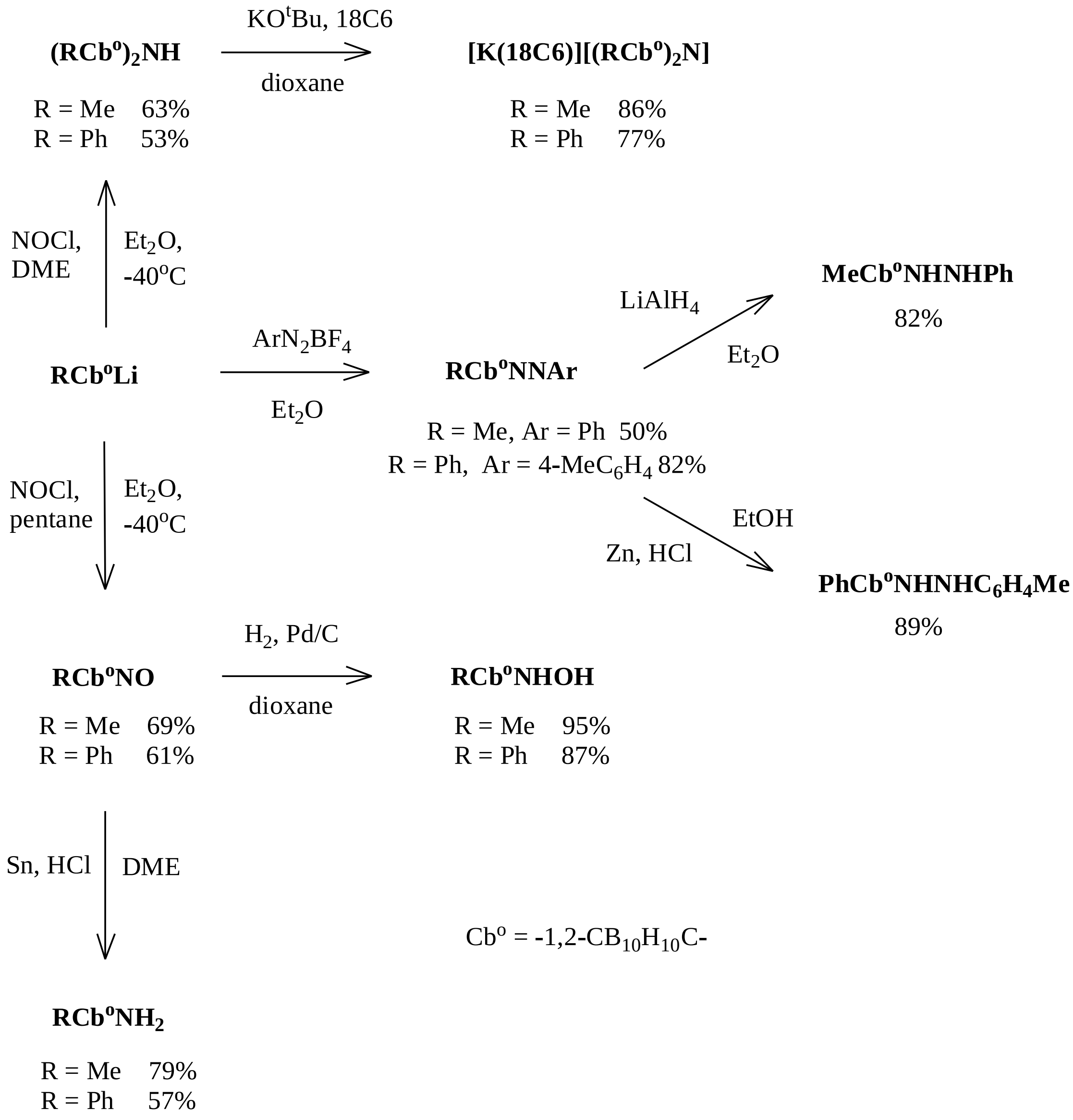

Scheme 1. Routes to carboranyl-nitrogen derivatives.

Structural Aspects: New experimentally determined structures

The azo-carborane $PhCb^{o}N_2$(*p*-tolyl) (1) and hydrazo-carboranes $PhCb^{o}NHNH$(*p*-tolyl) (2) and $MeCb^{o}NHNHPh$ (3)

The crystal structures of these three compounds were determined by X-ray diffraction (for details, see Experimental). Their molecular structures are illustrated in Figures 2 and 3.

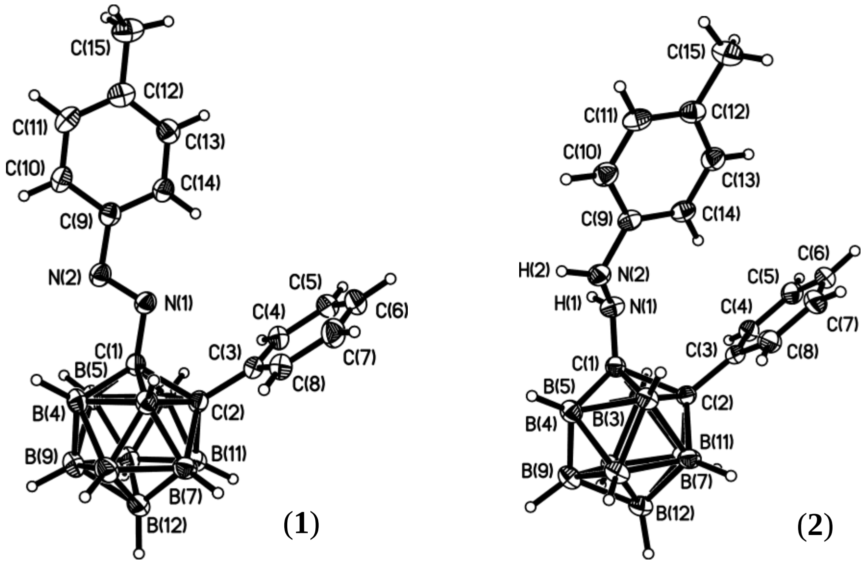

Figure 2. Molecular structures of $PhCb^{o}N_2C_6H_4Me$ (**1**) and $PhCb^{o}NHNHC_6H_4Me$ (**2**). Selected bond distances (Å) and angles (°) for (**1**): N(1)–N(2) 1.250(2); N(2)–C(9) 1.428(3); C(2)–C(3) 1.509(3); N(1)–N(2)–C(9) 112.88(15); N(1)–N(2)–C(9)–C(14) 15.3(3). For (**2**): N(1)–N(2) 1.409(2); N(2)–C(9) 1.421(3); C(2)–C(3) 1.497(3); N(1)–N(2)–C(9) 115.73(16); N(1)–N(2)–C(9)–C(14) −25.7(3).

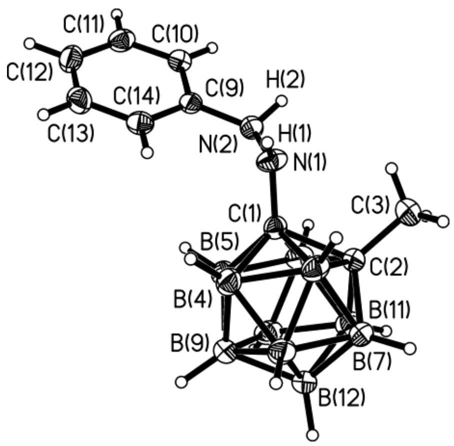

Figure 3. Molecular structure of $MeCb^{o}NHNHPh$ (**3**). Selected bond distances (Å) and angles (°): N(1)–N(2) 1.395(2), N(2)–C(9) 1.405(2), C(2)–C(3) 1.511(2), N(1)–N(2)–C(9) 119.17(13), N(1)–N(2)–C(9)–C(14) −19.0(2).

The structures of the azo-carborane (**1**) and its hydrazo analogue (**2**) (Figure 2) are similar, differing significantly, and as expected, only in the bond lengths and angles in the region of their –N=N– and –N(H)N(H)– units. Their NN links, at 1.250(2) in (**1**) and 1.409(2) Å in (**2**), are of normal length for double and single bonds respectively between nitrogen atoms. The CNN bond angles, at both ends of the N(1)–N(2) links, appear not to differ between the two ends (implying that the link to the carboranyl residue resembles that to the aryl group in both (**1**) and (**2**)) nor between (**1**) and (**2**), suggesting both (**1**) and (**2**) contain sp^2-hybridised nitrogen atoms. In both (**1**) and (**2**), the phenyl substituent on C(2) lies in a plane roughly perpendicular to the N(1)–C(1)–C(2) plane, as would be expected not only on steric grounds (to keep it away from the substituent on C(1)), but also as this is the orientation that optimises π-donation from ring to cage and causes *ca* 0.03 Å C1–C2 bond lengthening [15,16].

The orientations of the azo and hydrazo substituents on C(1), however, differ significantly. In (**1**), the azo N(1)–N(2)–C(9) unit lies in the N(1)–C(1)–C(2) plane, as in the nitroso carborane $PhCb^oNO$ studied previously [10]. In (**2**), the hydrazo N(1)–N(2)–C(9) unit is twisted out of the C(1)–C(2)–C(3) plane, clearly not on steric grounds, but to an extent that significantly ensures that the lone pair on N(1) lies in that plane. The view of (**2**) in Figure 2 shows the *ortho* hydrogen atom on C(14) lying over, and attracted to, the π-cloud of the phenyl group on C(2), with an H…centroid distance of 2.65 Å, and this attraction is likely to be responsible for the orientation of the tolyl group.

The molecular structure of compound (**3**), $MeCb^oNHNHPh$, shown in Figure 3, differs from that of (**2**) in the orientation of the aryl-hydrazo group, away from the methyl substituent on C(2). However, the local geometry about N(1) resembles that in (**2**) in ensuring that the lone pair on N(1) lies in the N(1)–C(1)–C(2) plane.

The hydroxylamino-carborane $PhCb^oNHOH$ (4)

The molecular structure of this compound (Figure 4) was determined by single-crystal studies on a dioxane hemisolvate of composition $PhCb^oNHOH{\cdot}0.5$dioxane. The orientations of both substituents on the carborane cage were found to resemble those already discussed for compounds (**2**) and (**3**), and are in line with those found previously for $PhCb^oNH_2$ [4]. The phenyl group in (**4**) lies roughly perpendicular to the N(1)–C(1)–C(2) plane, and the HNOH unit is oriented away from the phenyl group, like the HNNHR unit in (**2**), implying that the lone pair on the nitrogen lies in the N(1)–C(1)–C(2) plane. In the crystal structure, intermolecular N–H…O hydrogen-bonding interactions between the hydroxylamino units link the molecules into $(PhCb^oNHOH)_n$ chains, which in turn are interlinked by N–OH…O hydrogen bonds to both oxygen atoms of the dioxane molecules (Figure 5).

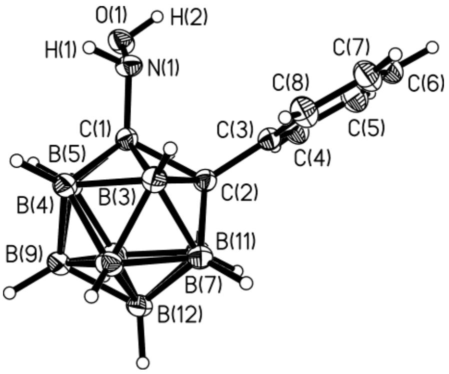

Figure 4. Molecular structure of $PhCb^oNHOH$ (**4**). The dioxane molecule in the crystal structure is not shown. Selected bond distances (Å) N(1)–O(1) 1.435(2); C(2)–C(3) 1.506(3).

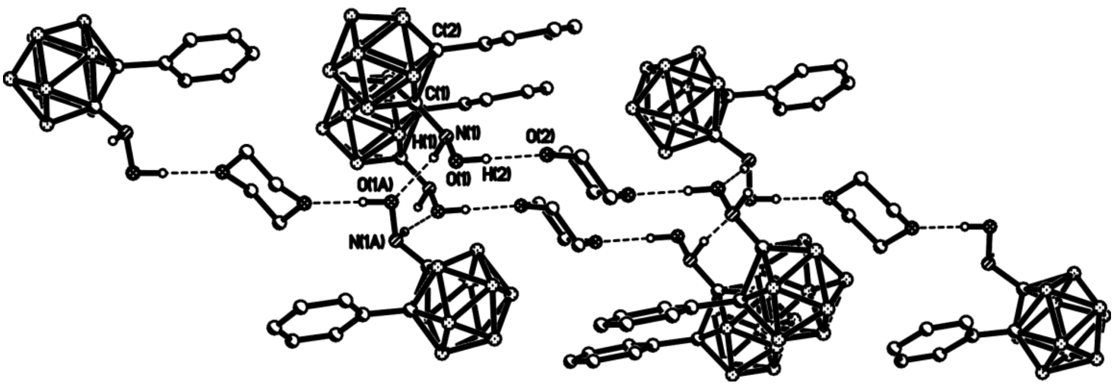

Figure 5. Supramolecular structure of $PhCb^oNHOH \cdot 0.5$dioxane. Selected intermolecular distances (Å) and angles (°): O(1)…O(2) 2.752(2), N(1)…O(1A) 3.209(2), O(1)–H(2)…O(2) 177(3), N(1)–H(1)…O(1A) 167(2). [O(1A) is generated from O(1) by screw-axis symmetry]

Structural Aspects: Structural characteristics of RCb^{o}N systems

The structures of the four compounds (**1**)–(**4**) described above, together with the four in our previous paper [10] [PhCb^{o}NO, (PhCb^o)$_2$NH, (MeCb^o)$_2$NH and the anion (PhCb^o)$_2$N$^-$] and the amine PhCb^{o}NH$_2$ characterised earlier [4], provide a useful data bank from which to deduce some common characteristics of *ortho*-carboranyl-nitrogen systems. These include preferred orientations of the *exo*-nitrogen substituent with respect to the carborane cage, and systematic complementary trends in their *exo*-C(1)–N(1) and cage C(1)–C(2) bond distances; as the former shorten, the latter lengthen.

The compounds we have studied are of two formula types, RCb^{o}NHR" and RCb^{o}N=Z. Their structures are shown in Figures 6 and 7. The nitroso- and azo-carboranes PhCb^{o}N=O and PhCb^{o}N=N(*p*-tolyl) are of the latter type [10]. All of the other compounds are of the former type, including the anion (PhCb^o)$_2$N$^-$ in which the lone pair left on deprotonation of the parent amine can be regarded as occupying the site vacated by hydrogen.

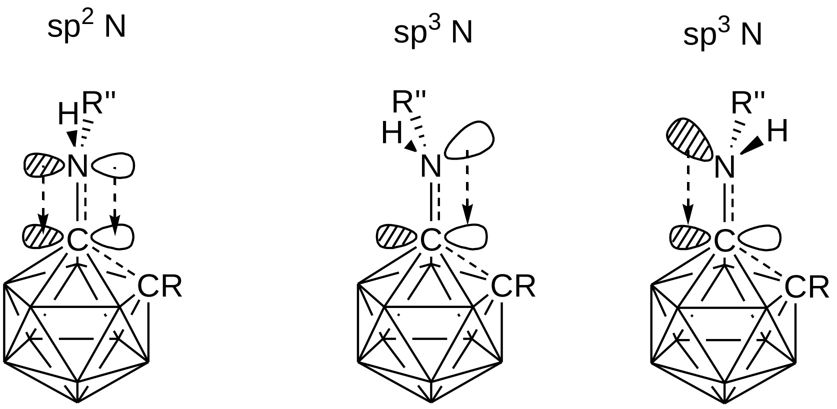

Figure 6. Preferred orientations in RCb^{o}NHR" systems. The cage acts as a π-acceptor.

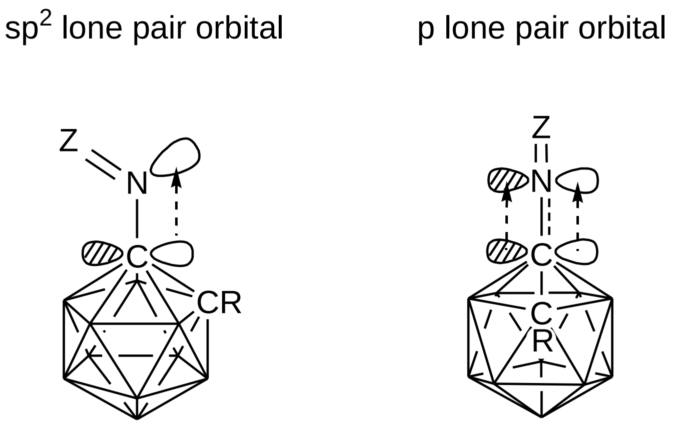

Figure 7. Preferred orientation in RCb^{o}N=Z systems (Z = O, NR'). The cage *may* act as a π-donor.

Table 1. X-ray-determined trends: the optimum torsion angle C(2)–C(1)–N(1)–Z/R" to align the *p*-orbital lone pair of sp^2-hybridised nitrogen with the cage C(1)–C(2) bond is 90° for compounds RCb^oNHR'', to align the sp^2-orbital lone pair of sp^2-hybridised nitrogen with the cage C(1)–C(2) bond is 180° for compounds $RCb^oN{=}Z$. HMPA = $OP(NMe_2)_3$.

$PhCb^oX$

X		C(1)–C(2) (Å)	C(1)–N(1) (Å)	C(2)–C(1)–N(1) (°)	C(1)–N(1)–Z/R" (°)	C(2)–C(1)–N(1)–Z/R" (°)	C(1)–C(2)–C(Ph)–C(Ph) (°)	Reference
NO		1.677(2)	1.490(2)	112.1(2)	113.0(2)	164.7	82.4	10
$N{=}NC_6H_4Me$		1.694(2)	1.443(2)	111.3(1)	112.8(2)	178.2	75.5	This work
NHOH		1.737(3)	1.423(3)	115.7(2)	110.7(2)	101.6	86.5	This work
NH_2 (4)	A	1.745(3)	1.391(3)	119.3(2)			69.9	4
	B	1.765(3)	1.403(3)	115.9(2)			91.2	
	C	1.774(3)	1.404(3)	119.8(2)			64.1	
	D	1.785(3)	1.392(2)	118.5(2)			76.7	
$NHNHC_6H_4Me$		1.778(3)	1.401(2)	115.2(2)	116.4(2)	105.9	83.4	This work
$NHCb^oPh$		1.794(3)	1.404(2)	117.3(2)	132.0(2)	92.4	70.1	10
		1.799(3)	1.404(2)	116.9(2)		97.6	73.9	
$NH_2\cdot$HMPA (2)	A	1.818(8)	1.360(8)	116.1(6)			59.3	4
	B	1.853(8)	1.363(9)	114.9(5)			81.8	
$[NCb^oPh]^-$		1.980(3)	1.355(4)	118.8(2)	127.0(2)	90.3	53.6	10
		1.995(3)	1.345(4)	118.8(2)		89.0	53.2	

$MeCb^oX$

X	C(1)–C(2) (Å)	C(1)–N(1) (Å)	C(2)–C(1)–N(1) (°)	C(1)–N(1)–Z/R" (°)	C(2)–C(1)–N(1)–Z/R " (°)	Reference
$NHCb^oMe$	1.748(4)	1.409(4)	117.3(2)	131.1(2)	95.0	10
	1.752(4)	1.410(4)	117.0(2)	131.1(2)	94.7	
NHNHPh	1.770(2)	1.388(2)	115.9(1)	118.8(1)	104.1	This work

Figures 6 and 7 show the NHR" and N=Z units in their preferred orientations about the *exo*-C(1)–N(1) bond with respect to the carborane cage, with the substituents R" or Z leaning away from the substituent R (Ph or Me) on the other cage carbon atom C(2). This orientation not only minimises steric non-bonding repulsive interactions between the groups on C(1) and C(2), but aligns the lone pair of electrons on the *exo*-nitrogen atom on C(1) in the C(2)–C(1)–N(1) plane for RCb^oNHR'', the alignment best suited for dative π-bonding from the nitrogen lone pair into the *p*-AO on C(1) responsible for cage C(1)–C(2) σ-bonding, as shown in Figure 6.

The extent to which *exo*-dative C=N π-bonding donation from the NHR" group occurs (and whether it does so at the expense of cage C(1)–C(2) σ-bonding) can be inferred from the experimental C(1)–C(2) and C(1)–N(1) distances in Table 1, in which compounds are listed in the order of their increasing cage C(1)–C(2) distances, which matches the sequence of decreasing C(1)–N(1) distances. Table 1 includes also torsion angles C(2)–C(1)–N(1)–Z/R ", which reveal that these compounds show some departures from the preferred orientations shown in Figures 6 and 7, bond angles C(2)–C(1)–N(1), which show expected deviations from a normal angle of 121.7° for an *exo*-bond on a regular icosahedron; and the C(1)–N(1)–Z/R" bond angles at nitrogen, which for species RCb^oNHR'' would be 120° for an ideal trigonal planar coordination at nitrogen (sp^2) and 109° for pyramidal nitrogen (sp^3). The data in Table 1 include the four distinct molecules of $PhCb^oNH_2$ in the asymmetric unit of the crystal structure and for the two distinct molecules of this same species in its hydrogen-bonded adduct with hexamethylphosphoramide, $PhCb^oNH_2 \cdot HMPA$ [4].

The range over which cage C(1)–C(2) bond distances vary in Table 1 (1.677(2) to 1.995(3) Å, i.e. 0.32 Å) is more than twice the range over which *exo*-C=N distances vary (1.490(2) to 1.345(4) Å i.e. 0.15 Å), because the former are fractional-order bonds becoming progressively weaker as the Table is descended, whereas the latter range in bond order from single to multiple. To aid comparison within the series, AM1 calculations have been carried out using the atomic coordinates determined by X-ray diffraction, without further optimisation. Selected bond distances and orders, with corresponding σ and π contributions, are given in Table 2.

Table 2. Observed bond distances (Å) and calculated bond orders

X	C(1)–C(2)	Bond Order	C(1)–N(1)	Bond Order	π-bond Order
		$PhCb^oX$			
NO	1.677(2)	0.605	1.490(2)	0.921	0.056
N=NAr	1.694(2)	0.590	1.444(2)	0.998	0.070
NHOH	1.737(3)	0.539	1.423(3)	1.025	0.073
NHNHAr	1.778(3)	0.485	1.401(2)	1.044	0.104
$NHCb^oPh$	1.798(3)	0.453	1.404(2)	1.038	0.124
NH_2 (C)	1.774(3)	0.456	1.404(3)	1.102	0.143
$NH_2\cdot$HMPA (av)	1.835(8)	0.396	1.362(8)	1.146	0.185
$[NCb^oPh]^-$	1.987(3)	0.235	1.350(4)	1.295	0.357
		$MeCb^oX$			
$NHCb^oMe$ (av)	1.750(4)	0.506	1.410(4)	1.026	0.113
NHNHPh	1.770(2)	0.486	1.387(2)	1.057	0.128

The data in Table 2 show the correlation between the cage C(1)–C(2) and *exo*-C(1)–N(1) bond orders expected from their lengths. The bond orders of the cage C…C bonds decrease as those of the *exo* C(1)–N(1) bonds increase. The range over which the C(1)–C(2) bond orders vary (from 0.61 in $PhCb^oNO$ to 0.24 in the anion $(PhCb^o)_2N^-$) is comparable to that over which the *exo* C(1)–N bond orders vary (from 0.92 to 1.30), and is itself worthy of comment. Because icosahedral carborane clusters are held together by only thirteen skeletal electron pairs spread around their thirty edge 'bonds', the average cage edge bond order will be 0.43 (13/30). The cage carbon–carbon bond in *ortho*-carborane HCb^oH itself has an order some 50% in excess of this because the carbon atoms are more electronegative than their boron neighbours and so attract a greater share of the electrons available. The data in Table 2 show that the cage C(1)–C(2) bond order has been reduced to about this average icosahedral value of 0.43 in the amine $PhCb^oNH_2$, and to roughly half this value in the anion $(PhCb^o)_2N^-$.

In our discussion of bond lengths and bond order so far, we have concentrated on the cage C(1)–C(2) and *exo* C(1)–N(1) bonds. This is because these are the only bonds in these systems $PhCb^oX$ whose lengths and orders change significantly and systematically with X, as illustrated by the data in Table 3, which lists the experimental lengths of all the 2-centre links in the immediate environment of C(1); Figure 8 illustrates that pentagonal pyramidal environment. From Table 3 it is clear that, although there are minor variations between compounds in the measured lengths of C(1)–B(3/6), C(1)–B(4,5), C(2)–B(3,6), B(3,6)–B(4,5) and B(4)–B(5), these variations cannot be regarded as systematic or significant.

However, on closer inspection, the C1–C2 bond lengths determined cannot simply be explained by the orientation of the π-donating groups. For example, the two compounds **2** and **3** contain similar C1–C2 bond lengths of *ca* 1.77 Å even though it is generally accepted that the phenyl group lengthens the bond by *ca* 0.03–0.05 Å compared to the methyl group due to the steric and/or electronic effect(s) of the former[17]. The difference of 0.04 Å for the C1–C2 bond lengths in **2** and **4** is significant even though the orientations of the nitrogen groups are similar. There are six distinct $PhCb^oNH_2$ molecular geometries experimentally determined, with C1–C2 bond lengths ranging from 1.745 to 1.853 Å (see Table 1) – a difference of 0.11 Å, which cannot be explained solely by the orientation of the amine group.

Table 3. Interatomic distances (Å) and torsion angles (°) for compounds $PhCb^oX$

X	C1–C2	C1–N	C1–B3/6	C1–B4/5	C2–B3/6	B3/6–B4/5	B4–B5
H [18]	1.643(1)		1.713(1)	1.695(1)	1.733(1)	1.776(1)	1.781(1)
NO	1.677(2)	1.490(2)	1.706(2)	1.703(2)	1.740(2)	1.786(3)	1.779(3)
NNAr	1.694(2)	1.443(2)	1.716(3)	1.703(3)	1.738(3)	1.780(3)	1.784(3)
NHOH	1.737(3)	1.423(3)	1.721(3)	1.701(3)	1.732(3)	1.779(3)	1.781(3)
NHNHAr	1.778(3)	1.401(2)	1.719(3)	1.708(3)	1.736(3)	1.786(3)	1.784(3)
NH_2 (av)	1.767(3)	1.396(3)	1.715(4)	1.698(4)	1.722(4)	1.780(4)	1.775(4)

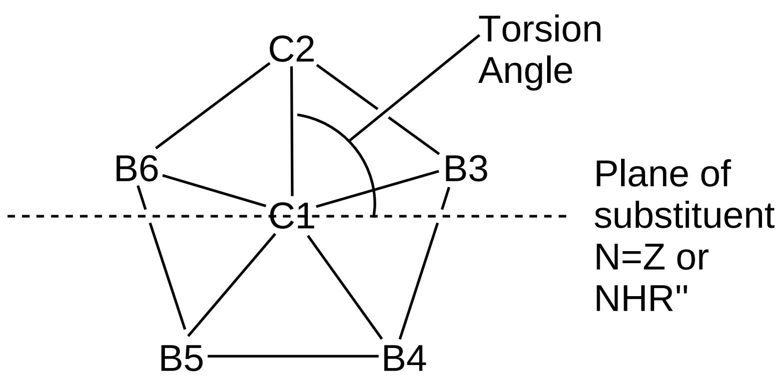

Figure 8. The pentagonal pyramidal environment about C1

Structural Aspects: Computational studies

Optimised geometries of carboranes at the MP2/6-31G* level of theory have been shown to be in excellent agreement with experimental geometries determined by gas-phase electron diffraction [19] and X-ray crystallography [4,8,15,20]. Earlier, we had carried out computations on model geometries of HCb^{o}X with π-donor groups (X = OH, NH^-, NH_2 and CH_2^-) to investigate the effect of orientation of these groups on the C1–C2 bond length; in these computations a planar configuration (sp^2) was assumed for NH_2 [4]. The effect of a pyramidal form (sp^3) at a nitrogen π-donor group on the C1–C2 bond or the effect of π-acceptor groups on the cage geometry had not been investigated previously. Here, data for the systems HCb^{o}X where X = N=O, N=NH, NHOH, NH_2 and $NHNH_2$ in various possible orientations (indicated by their torsion angles) are listed in Table 4. The pyramidal or planar configurations of the nitrogen atom N1 attached to C1 for NHR" groups were also examined.

The model carboranes with acceptor groups, NO and NNH, prefer to be oriented in plane (0° and 180°) with the C1–C2 bond, as opposed to being oriented perpendicular to the C1–C2 bond, with an energy difference of *ca* 4 kcal mol^{-1} (Figure 8). The reason for the slight preference for 0° orientations over 180° orientations in these models is the favourable cage C–H…X bond interactions [8]. Energetically, the hydroxylamine (NHOH) group clearly favours the pyramidal form (sp^3 N) over the planar form (sp^2 N) irrespective of the orientation. There is no strong preference for one orientation over another for the NHOH group. The substituents NO, NNH and NHOH (with sp^3 N) have little orientational influence on the *ortho*-carborane cage geometry.

Table 4. Selected bond lengths (Å) and energies of MP2-optimised geometries of HCb^{o}X where torsion angles for C2–C1–N–Z/R" are fixed at 0, 90 and 180°. (a = N–H away from C1, t = N–H towards C1)

X		N1–Z/R"	C1–N1	C1–C2	C1–B3/6	C1–B4/5	Energy (au)	Relative E (kcal mol^{-1})
NO	0	1.230	1.491	1.621	1.713	1.691	–459.79796	0.0
	90	1.227	1.514	1.618	1.716	1.689	–459.79160	4.1
	180	1.228	1.493	1.617	1.711	1.692	–459.79740	0.2
NNH	0	1.265	1.455	1.634	1.716	1.694	–439.98786	0.0
	90	1.265	1.468	1.621	1.725	1.693	–439.98075	4.7
	180	1.265	1.457	1.624	1.715	1.698	–439.98616	1.1
NHOH(sp^3)	0	1.445	1.450	1.631	1.712	1.693	–460.99182	0.0
	90(a)	1.440	1.441	1.635	1.727	1.699	–460.99040	0.1
	90(t)	1.437	1.434	1.665	1.723	1.697	–460.98922	1.7
	180	1.441	1.452	1.620	1.731	1.699	–460.98794	2.6
NHOH(sp^2)	0	1.396	1.397	1.609	1.749	1.704	–460.97107	13.0
	90	1.397	1.377	1.739	1.720	1.700	–460.97564	10.0
	180	1.394	1.396	1.607	1.756	1.706	–460.96728	15.6
NH_2(sp^3)	0	1.019	1.430	1.640	1.731	1.700	–386.01371	4.1
	90(a)	1.017	1.422	1.651	1.722	1.702	–386.01982	0.0
	90(t)	1.015	1.412	1.675	1.725	1.700	–386.01982	0.0
	180	1.020	1.434	1.623	1.732	1.701	–386.01650	2.2

NH_2 (sp^2)	0	1.007	1.396	1.612	1.752	1.705	–386.00656	8.9
	90	1.008	1.383	1.713	1.718	1.703	–386.01552	2.9
$NHNH_2$(sp^3)	0	1.417	1.442	1.636	1.728	1.701	–441.16414	3.9
	90(a)	1.420	1.429	1.654	1.725	1.701	–441.16998	0.0
	90(t)	1.416	1.414	1.703	1.724	1.699	–441.16752	1.6
	180	1.428	1.445	1.623	1.736	1.701	–441.16800	1.3
$NHNH_2$(sp^2)	0	1.389	1.406	1.612	1.748	1.705	–441.15795	8.0
	90	1.399	1.386	1.731	1.721	1.701	–441.16639	2.4
	180	1.395	1.403	1.611	1.755	1.706	–441.15887	7.4

By contrast, the models containing the NH_2 groups are similar in energy irrespective of whether the nitrogen atom N1 is planar (sp^2) or pyramidal (sp^3) in configuration (Figure 7). However, the 90° orientations are energetically favourable and are expected for a π-donor group -NHR" to be oriented to align the donor p-orbital with the C1–C2 bond for maximum overlap. The model HCb^oNH_2 has four geometries within a range of 2.9 kcal mol^{-1} in energy but their C1–C2 bond distances vary from 1.623 to 1.713 Å, a difference of 0.09 Å, attributable to the orientations and the sp^2 or sp^3 configuration about the nitrogen atom. Similar observations are found for the model carborane containing the $NHNH_2$ group.

There are parallels here between carborane chemistry and aromatic ring chemistry, where substituents that can act as π-donors or π-acceptors adopt orientations that maximise interaction with the π-system of the aromatic ring (Figure 9) provided that steric factors do not rule out the preferred orientations of substituents NO, NNH, NHOH, NH_2 and $NHNH_2$ when attached to a benzene ring. Selected bond distances and relative energies from computational data on these benzene derivatives for the two orientations, planar (0°) and perpendicular (90°), at the MP2/6-31G* level of theory are listed in Table 5. For the acceptor groups NO and NNH, the planar form is energetically preferred over the perpendicular form by 8.9 and 5.1 kcal mol^{-1} respectively, but the orientation has little influence on the ring geometries [21]. The NHOH group strongly favours the pyramidal (sp^3) configuration over the planar (sp^2) form energetically, but small energy and geometry differences between the two orientations are found for the sp^3 form. The amine NH_2 group does not have a strong energetic preference for the sp^2 or sp^3 form but has a notable orientational effect on the C–N bond, with distances of 1.381 Å for the sp^2 N geometry in plane with the C1–C2 bond (0°) and 1.435 Å for the sp^3 N geometry perpendicular to the C1–C2 bond (90°) [22]. The ring geometry, however, remains largely unaffected by the C–N bond variations. The orientation of the $NHNH_2$ group has a similar effect on the geometry and energies as the orientation of the NH_2 group. Preferred orientations determined computationally for PhNNH and $PhNHNH_2$ are in accord with the orientations of the aromatic rings in the experimental structures for **1**, **2** and **3**.

Figure 9. Preferred orientations in PhNHR" and PhN=Z systems

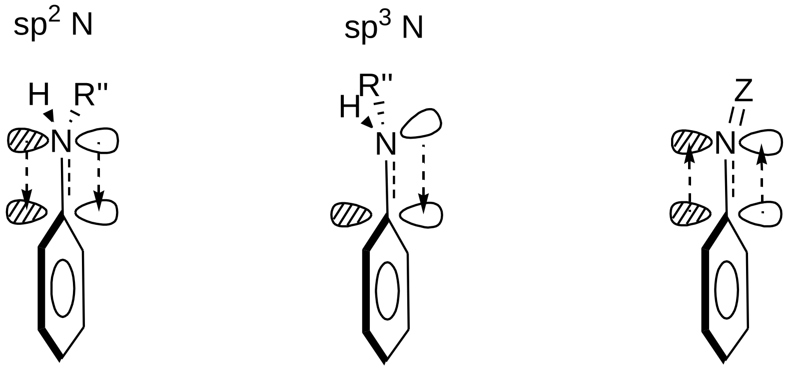

Table 5. Selected bond lengths (Å) and energies of MP2-optimised geometries of PhX where torsion angles for C2–C1–N–Z/R" are fixed at 0 and 90°.

X		N1–Z/R"	C1–N1	C1–C2	Relative Energy (kcal mol^{-1})
NO	0	1.244	1.443	1.399	0
	90	1.243	1.460	1.394	8.9
NNH	0	1.272	1.433	1.399	0
	90	1.270	1.441	1.395	5.1
NHOH(*sp*^{3})	0	1.440	1.432	1.399	0
	90	1.465	1.434	1.398	1.5
NHOH(*sp*^{2})	0	1.395	1.378	1.403	7.5
	90	1.412	1.408	1.403	16.9
NH_2(*sp*^{3})	0	1.014	1.409	1.403	0
	90	1.019	1.435	1.401	2.4
NH_2(*sp*^{2})	0	1.007	1.381	1.405	1.2
	90	1.005	1.416	1.403	9.2
$NHNH_2$(*sp*^{3})	0	1.410	1.404	1.404	0.0
	90	1.449	1.432	1.401	1.8
$NHNH_2$(*sp*^{2})	0	1.396	1.386	1.404	2.4
	90	1.403	1.415	1.402	12.4

The geometries of $PhCb^oX$ and $MeCb^oX$ were also computed at the MP2/6-31G* level of theory. Comparisons shown in Table 6 reveal very good agreements between the selected geometric parameters for optimised and experimental geometries in all cases. The NHR" groups, as discussed for the model carboranes, are particularly intriguing: the sp^3 N form is more stable than the sp^2 N form in these groups. However, for the NH_2 group the energy difference between the geometries containing sp^3 N and sp^2 N groups is small (less than 3 kcal mol^{-1}), which indicates that both forms could co-exist in the solid and solution states where intermolecular interactions come into play. The computed C1–C2 distances of 1.743 and 1.813 Å for the sp^3 N and sp^2 N $PhCb^oNH_2$ geometries respectively, and their energies, are in broad agreement with the observation of six distinct $PhCb^oNH_2$ molecules with C(1)–C(2) bond distances of 1.745 to 1.853 Å (see Table 1) in the crystal structure.

For compounds with NHNHR' groups, **2** and **3**, the relative energies between their sp^3 N and sp^2 N geometries are slightly larger at *ca* 4.0 kcal mol^{-1}, but comparison of the bond parameters of experimental geometries with sp^3 N optimised geometries are poor. The experimental geometry for **3** is in much better agreement with the sp^2 N optimised geometry of $MeCb^oNHNHPh$, whereas the experimental geometry for **2** lies between the two optimised geometries (sp^2 N and sp^3 N) of $PhCb^oNHNHC_6H_4Me$. As for $PhCb^oNH_2$, these geometries depend on intermolecular interactions such as crystal packing forces. This subtle difference in the sp^2/sp^3 N character results in similar C1–C2 bond distances found experimentally for **2** and **3**. The pyramidal sp^3 N form is clearly favoured in energy for the $PhCb^oNHOH$ geometry and in accord with the experimental geometry found for **4**.

The optimised and experimental geometries for the dicarboranylamines $(PhCb^o)_2NH$ and $(MeCb^o)_2NH$ are in excellent agreement and their planar nitrogen atoms are clearly sp^2 in character. Optimised geometries for some methyl analogues, where no experimental structures were determined, reveal geometries and trends similar to the experimental and optimised geometries for the phenyl analogues.

Table 6. Comparison of selected computed and experimental geometric parameters (Å and °) for RCb^{o}X systems. Experimental values are shown in italics.

						PhCb^{o}X	
X		C1–C2	C1–N1	C2–C1–N1	C1–N1–X/R "	Angle sum at N	Relative Energy (kcal mol^{-1})
H		1.636					
		1.643(1)					
NO		1.671	1.490	112.1	111.6		
		1.677(2)	*1.490(2)*	*112.1(2)*	*113.0(2)*		
N=NC$_6$H$_4$Me		1.679	1.441	111.1	111.3		
		1.694(2)	*1.444(2)*	*111.3(1)*	*112.8(2)*		
NHOH	*sp*^{3}	1.719	1.430	113.5	110.6	322.4	0.0
	sp^2	1.828	1.367	116.2	120.9	360.0	8.3
		1.737(3)	*1.423(3)*	*115.7(2)*	*110.7(2)*	*324.7*	
NHCb^{o}Ph		1.790	1.401	115.9	132.3	360.0	
		1.798(3)	*1.404(2)*	*117.3(2)*	*132.0(2)*	*360.0*	
NHNHC$_6$H$_4$Me	*sp*^{3}	1.727	1.424	116.4	117.4	335.4	0.0
	sp^2	1.830	1.379	119.1	120.5	360.0	4.2
		1.778(3)	*1.401(2)*	*115.2(2)*	*116.4(2)*	*342.4*	
NH$_2$	*sp*^{3}	1.743	1.411	114.5		332.7	0.0
	sp^2	1.813	1.374	117.0		360.0	2.6
		1.767(3)	*1.396(3)*	*118.4(2)*		*344.3*	
[NCb^{o}Ph]$^{-}$		1.977	1.353	118.7	126.2		
		1.987(3)	*1.355(4)*	*118.8(2)*	*127.0*		

MeCb^{o}X

X		C1–C2	C1–N1	C2–C1–N1	C1–N1–X/R "	Angle sum at N	Relative Energy (kcal mol^{-1})
H		1.630					
NO		1.638	1.488	112.5	111.9		
N=NPh		1.644	1.444	112.2	110.9		
NHOH	*sp*^{3}	1.696	1.427	115.4	113.2		0.0
	sp^{2}	1.774	1.374	118.2	120.7		6.0
NHCb^{o}Me		1.748	1.406	117.3	132.3	360.0	
		1.750(4)	*1.410(4)*	*117.2(2)*	*131.1(2)*	*359.8*	
NHNHPh	*sp*^{3}	1.737	1.448	114.5	119.9	338.9	0.0
	sp^{2}	1.764	1.384	117.9	121.6	360.0	3.8
		1.770(2)	*1.387(2)*	*115.9(1)*	*118.8(1)*	*355.4*	
NH_2	*sp*^{3}	1.683	1.420	114.9		330.0	0.0
	sp^{2}	1.770	1.379	118.0		360.0	2.7
[NCb^{o}Me]$^{-}$		1.886	1.358	118.7	126.2		

Experimental and computed NMR trends

The ^{11}B NMR spectra of polyhedral borane clusters such as carboranes provide a rich source of information provided that signals can be assigned with confidence. At the simplest level, the number of different boron sites in a molecule, deduced from the number of resonances, helps identify isomers. Of more importance in the present context is the 'antipodal effect' in icosahedral carborane chemistry [23], whereby the NMR shift of the boron atom directly opposite a substituted cage carbon atom is sensitive to the nature of the substituent. In *ortho*-carborane derivatives RCb^oX, bearing substituents X and R on carbon atoms 1 and 2 respectively, the resonances of the atoms opposite (B12 and B9 respectively) respond to the corresponding substituent, particularly if that substituent is a π-donor [2,4]. For the present series of compounds RCb^oX, where X is a nitrogen π-donor, the antipodal shift is expected to be related to the degree of *exo* π-bonding, and hence to *exo* C1–N1 and cage C1–C2 bond lengths.

For such a comparison to be made the ^{11}B NMR shift for the antipodal atom (^{11}B δ-B12) must be reliably assigned. Although the two peaks corresponding to B9 and B12 are readily identified from the peak intensities it is impossible to assign each unambiguously without assumptions being made. One of these peaks appears at approximately the same shift in all compounds. This therefore can be assigned to B9, antipodal to the Ph or Me group in $PhCb^oX$ and $MeCb^oX$ respectively. This peak would be expected to change little in these series of compounds as the substituent on C2, i.e. the Me or Ph group, remains unchanged. ^{11}B NMR shifts for B9 and B12 have been assigned on this basis (see Table 7).

The antipodal shift increases as π-bonding increases, displayed by the graph of the B12 shift vs experimental C–N bond lengths (Figure 10). This is in agreement with previous work showing that such shifts are related to electron donation to the cluster. Hence the ^{11}B NMR data give an indication of degree of *exo* π-bonding and this can be used to assess such effects in compounds which have not been structurally characterised.

Table 7. Comparison of selected experimental (in $CDCl_3$) and computed NMR shifts (ppm) for RCb^{o}X systems. Calculated values are in italics.

PhCb^{o}X

X	δ(B12)		δ(B12H)		δ(C1)		δ(C2)	
H [4]	–1.2	*–1.2*	2.46	*3.09*	60.1	*57.7*	76.5	*78.5*
NO	–2.0	*0.2*	2.67	*3.34*	114.1	*125.1*	81.3	*84.1*
N=NC_6H_4Me	–4.2	*–2.4*	2.57	*3.18*	98.8	*103.8*	81.7	*83.0*
NHOH^{a}	–5.5	*–4.5*	2.38	*3.00*	98.4	*101.0*	86.5	*87.8*
NHCb^{o}Ph	–5.8	*–5.1*	2.28	*2.86*	94.4	*95.7*	90.3	*92.5*
NHNHC_6H_4Me^{b}	–6.8	*–6.0*	2.32	*2.85*	102.3	*105.3*	90.0	*91.3*
NH_2^{b}	–8.3	*–7.8*	2.18	*2.80*	96.3	*98.1*	87.7	*92.2*
[NCb^{o}Ph]$^{-\,c}$	–12.6	*–13.6*	1.72	*2.08*	129.5	*125.4*	89.8	*95.5*

MeCb^{o}X

X	δ(B12)		δ(B12H)		δ(C1)		δ(C2)	
H [24]	–1.7	*0.0*	2.31	*3.05*	61.5	*58.6*	70.4	*70.5*
NO	–2.4	*0.4*	2.50	*3.29*	111.4	*120.2*	73.3	*74.6*
N=NPh	–4.2	*–2.6*	2.40	*3.07*	95.7	*97.9*	73.9	*73.8*
NHOH^{a}	–6.1	*–5.8*	2.24	*2.83*	94.5	*96.6*	78.6	*81.8*
NHCb^{o}Me	–6.4	*–6.0*	2.22	*2.78*	90.9	*93.0*	81.8	*84.0*
NHNHPh^{b}	–7.1	*–6.5*	2.16	*2.81*	96.7	*98.9*	80.9	*82.2*
NH_2^{b}	–9.4	*–8.4*	1.98	*2.90*	91.1	*92.5*	78.9	*81.0*
[NCb^{o}Me]$^{-\,c}$	–13.7	*–14.4*	1.59	*1.99*	120.0	*119.1*	87.0	*90.8*

^{a}Computed shifts for *sp*^{3} geometry
^{b}Computed shifts averaged for both *sp*^{2} and *sp*^{3} geometries
^{c}Observed values in CD_3CN

Figure 10. Correlation between the observed ^{11}B shift of B12 (ppm) and the experimental C(1)–N(1) bond length (Å)

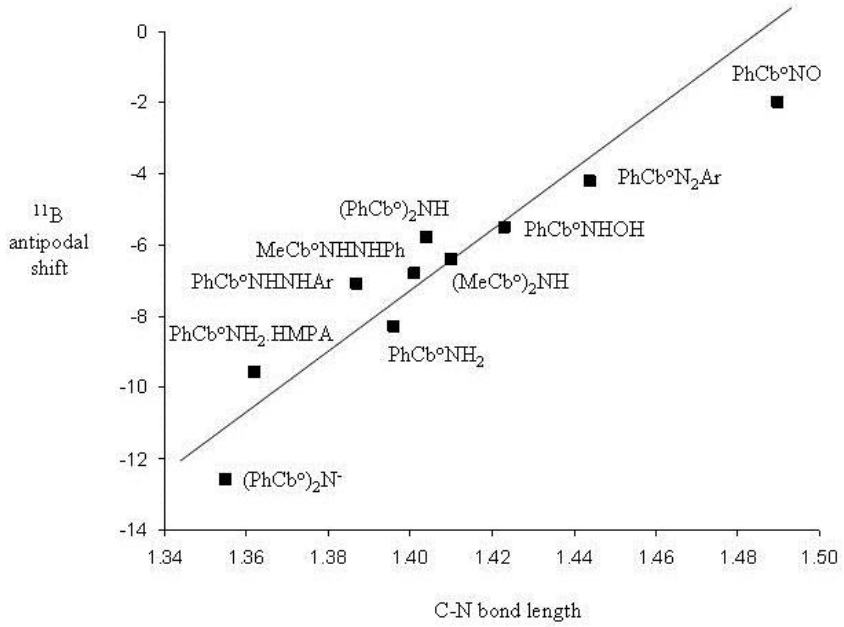

The shifts of the BH protons revealed by $^{1}H\{^{11}B\}$ NMR can be assigned using ^{1}H-^{11}B HETCOR or $^{1}H\{^{11}B$ selective$\}$ experiments. The ^{1}H shifts of the hydrogen atoms bonded to the antipodal boron show the same relationship with the C–N bond length as the ^{11}B shifts of B12, decreasing frequency of the antipodal hydrogen with increased π-bonding to the cage suggesting increased shielding. The ^{13}C shifts of the cage carbon atoms C1 and C2, however, are not simply related to the *exo*-C–N π-bonding effects. Calculated NMR chemical shifts on MP2-optimised geometries are in very good agreement with observed shifts and trends as shown in Table 7.

Conclusions

In this paper we have reported the crystallographically derived molecular structures and ^{11}B, ^{13}C and ^{1}H NMR spectra of four new *ortho*-carboranyl-nitrogen compounds PhCb^{o}N=N(*p*-tolyl) (**1**), PhCb^{o}NHNH(*p*-tolyl) (**2**), MeCb^{o}NHNHPh (**3**) and PhCb^{o}NHOH (**4**) (Cb^{o} = 1,2-$C_2B_{10}H_{10}$). Together with other carboranyl-nitrogen systems RCb^{o}X reported earlier, these provide a useful data bank from which the general structural, bonding and NMR characteristics of such systems can be discerned. Their structures show how dative exo C=N *p*-bonding from the substituent to the cage is reflected in shortening of the exo C–N bond (as it gains multiple character) and lengthening of the cage C1–C2 bond (as it loses bond order) to an extent that reflects the π-donor power of the substituent, the orientation of the CN group and the *sp*^{2} or *sp*^{3} character of the nitrogen atom for the NHR" group, which are seen from computational studies to be important. The ^{11}B NMR chemical shift of the boron atom antipodal to the substituent also provides a guide to the π-donor power of X.

Experimental Section

All air-sensitive manipulations were carried out under dry, oxygen-free N_2. Stirring refers to use of a magnetic stirrer. Hexanes were distilled over Na. 1,2-Dimethoxyethane (DME) was dried by reflux and distillation over potassium; ether refers to diethyl ether dried, where appropriate, over sodium. Ether solutions were dried over magnesium sulfate and evaporated near room temperature. 1-Methyl-*ortho*-carborane [25] and 1-phenyl-*ortho*-carborane [26] were prepared by literature methods and dried by sublimation at 0.01 mm Hg. 1-Nitroso-2-methyl-*ortho*-carborane and 1-nitroso-2-phenyl-*ortho*-carborane were made as described elsewhere [10]. Benzenediazonium tetrafluoroborate and 4-methylbenzenediazonium tetrafluoroborate salts were made using a general literature method [27].

Melting points were measured in capillary tubes with an Electrothermal 9200 heating block. Infrared spectra were recorded from KBr discs on Perkin Elmer 1600 series FTIR or Perkin Elmer 1720X FTIR spectrometers and ultraviolet spectra with a Shimadzu UV 1201. Elemental carbon, hydrogen and nitrogen analyses were performed using Exeter Analytical CE-440 or Carlo Erba Strumentazione EA Model 1106 instruments. Mass spectra (MS) were recorded on a VG Micromass 7070E instrument under EI conditions at 70 eV. Values of M show the isotope range $^{10}B_n$ to $^{11}B_n$ including a ^{13}C contribution if observed. NMR spectra were measured using Varian Unity-300 (^{1}H, ^{11}B, ^{13}C), Bruker AM250 (^{1}H, ^{13}C), Bruker Avance 400 (^{1}H, ^{11}B, ^{13}C) and/or Varian Inova 500 (^{1}H, ^{11}B) instruments. All chemical shifts are reported in δ (ppm) and coupling constants in Hz. ^{1}H NMR spectra were referenced to residual protio impurity in the solvent ($CDCl_3$, 7.26 ppm). ^{13}C NMR spectra were referenced to the solvent resonance ($CDCl_3$, 77.0 ppm). ^{11}B NMR spectra were referenced externally to $Et_2O{\cdot}BF_3$, $\delta = 0.0$ ppm. Peak assignments of cage boron and hydrogen atoms were determined with the aid of 2D $^{11}B\{^1H\}$-$^{11}B\{^1H\}$ COSY, selective $^1H\{^{11}B\}$ and ^1H-^{11}B correlation spectra.

Preparation of azocarboranes (modification of a reported [12] method)

A solution of the substituted lithiocarborane was prepared by the addition of butyllithium (5.05 ml, 2.5M in hexanes) to a solution of the starting carborane (0.0127 mol) in diethyl ether (100 ml) at 0°C. The solution was warmed to ambient temperature with stirring for 30 min. The diazonium salt was added as a solid over a period of 30 min and stirred overnight to give a cloudy red solution. Water was added and the organic layer was separated and washed with water. The organic layer was dried and evaporated to leave a brown residue. This was recrystallised from hexane to give orange crystals of the azocarborane.

1-Methyl-2-phenylazo-*ortho*-carborane, 1.78 g (50%), M.p. 122.5–123.5°C (lit. [12] 121–122°C). Found: C, 41.1; H, 7.0; N, 10.6. $C_9H_{18}B_{10}N_2$ requires C, 41.2; H, 6.9; N, 10.7%. IR ν_{max} (KBr) [cm^{-1}]: 3062w (aryl CH), 2926w (methyl CH), 2640m, 2615s, 2582s, 2574s, 2550s (BH), 1497s, 1451s, 1205s, 1157s, 1072s, 1019s, 768s, 728s, 683s, 419s. $^1H\{^{11}B\}$ NMR ($CDCl_3$), δ: 7.81 (d, 2H, *ortho*-phenyl CH), 7.58 (t, 1H, *para*-phenyl CH), 7.52 (d, 2H, *meta*-phenyl CH), 2.50 (s, 2H, H8,10), 2.40 (s, 5H, BH including H12), 2.30 (s, 3H, CH_3), 2.20 (s, 3H, BH); $^{11}B\{^1H\}$ NMR ($CDCl_3$), δ: –4.2 (1B, B12), –6.4 (1B, B9), –10.6 (8B); ^{13}C NMR ($CDCl_3$), δ: 151.2 (C_6H_5 *ipso*), 133.5 (d of t, $^1J_{CH}$ 161 Hz, $^2J_{CH}$ 8 Hz, C_6H_5 *para*), 129.4 (d of d, $^1J_{CH}$ 161 Hz, $^2J_{CH}$ 8 Hz, C_6H_5 *ortho*), 123.6 (d of t, $^1J_{CH}$ 161 Hz, $^2J_{CH}$ 6 Hz, C_6H_5 *meta*), 95.7 (C1), 73.9 (C2), 22.5 (q, $^1J_{CH}$ 132 Hz, CH_3).

1-Phenyl-2-(4-methylphenyl)azo-*ortho*-carborane, 2.77 g (82%), M.p. 90–91°C. Found: C, 53.1; H, 6.8; N, 8.1. $C_{15}H_{22}B_{10}N_2$ requires C, 53.3; H, 6.5; N, 8.3%. MS (EI^+, *m/z*) 91 (C_6H_4Me); 216–221 $[PhCb]^+$; IR ν_{max} (KBr) [cm^{-1}]: 3052w (aryl CH), 2922w (methyl CH), 2642m, 2603s, 2566s (BH), 1600s, 1500s, 1489s, 1472s, 1446s, 1157s, 1071s, 1026s, 827s, 810s, 802s, 752s, 688s. $^1H\{^{11}B\}$ NMR ($CDCl_3$), δ: 7.70 (d, 2H, *ortho* C_6H_5), 7.42 (t, $^3J_{HH}$ 8 Hz, 1H, *para* C_6H_5), 7.34 (t, $^3J_{HH}$ 8 Hz, 2H, *meta* C_6H_5), 7.35 (d, $^3J_{HH}$ 8 Hz, 2H, *meta* C_6H_4Me), 7.17 (d, $^3J_{HH}$ 8 Hz, 2H, *ortho* C_6H_4Me), 3.00 (s, 2H, BH), 2.63 (s, 2H, BH), 2.57 (s, 3H, BH), 2.44 (s, 1H, BH), 2.37 (s, 3H, CH_3), 2.34 (s, 2H, H9,12); $^{11}B\{^1H\}$ NMR ($CDCl_3$), δ: −4.2 (2B, B9,12),

−11.0 (8B); ^{13}C NMR ($CDCl_3$), δ: 149.1 (C–N), 144.4 (<u>C</u>–CH_3), 131.1 (*ortho* C_6H_5), 130.5 (*ipso* C_6H_5), 130.2 (*para* C_6H_5), 129.8, 128.2 (aryl CH); 123.5 (<u>C</u>HCN), 98.8 (C1), 81.7 (C2), 21.6 (CH_3).

Preparation of hydrazocarboranes

Lithium aluminium hydride, $LiAlH_4$, (0.3g, 8 mmol), was added to a solution of 1-methyl-2-phenylazo-*ortho*-carborane (0.50g, 1.91 mmol) in diethyl ether (20 ml) and the mixture stirred for 20 h. Wet diethyl ether was added, followed by water (10ml) and dilute HCl until the cloudy solution became clear. The organic layer was washed with water (2 × 50ml), dried and evaporated to leave a pale yellow solid. This was recrystallised from hot hexane to yield colourless crystals of 1-methyl-2-phenylhydrazo-*ortho*-carborane (0.41g, 82%). M.p. 142–144°C (lit. [12] 143–144 °C). Found: C, 40.7; H, 7.8; N, 10.3. $C_9H_{20}B_{10}N_2$ requires C, 40.9; H, 7.6; N, 10.3%. MS (EI$^+$, *m*/*z*) [M]$^+$ 260–267; 264 (100); IR ν_{max} (KBr) [cm^{-1}]: 3360, 3322 (NH), 3125 (phenyl CH), 2933 (methyl CH), 2615s, 2580s, 2559s (BH), 1601, 1497, 1454m, 1251m, 1019m, 754s, 696m. ^{1}H{^{11}B} NMR ($CDCl_3$), δ: 7.24 (t, $^3J_{HH}$ 7 Hz, 2H, *meta* C_6H_5), 6.90 (t, $^3J_{HH}$ 7 Hz, 1H, *para* C_6H_5), 6.85 (d, $^3J_{HH}$ 8 Hz, 2H, *ortho* C_6H_5), 5.68 (s, 1H, NH), 4.89 (s, 1H, NH), 2.52 (s, 2H, H8,10), 2.23 (s, 3H, BH), 2.16 (s, 3H, BH), 2.09 (s, 3H, CH_3), 2.05 (s, 2H, BH); ^{11}B{^{1}H} NMR ($CDCl_3$), δ: −6.1 (1B, B9), −7.1 (1B, B12), −11.0 (4B), −11.8 (4B); ^{13}C NMR ($CDCl_3$), δ: 147.3 (C_6H_5 *ipso*), 129.3 (d, $^1J_{CH}$ 158 Hz, C_6H_5), 121.0 (d, $^1J_{CH}$ 160 Hz, C_6H_5), 113.0 (d of t, $^1J_{CH}$ 156 Hz, C_6H_5), 96.7 (C1), 80.9 (C2), 22.1 (q, $^1J_{CH}$ 130 Hz, CH_3).

The compound 1-phenyl-2-(4-methylphenyl)azo-*ortho*-carborane (0.73 g) was dissolved in 20 ml of ethanol. Zinc dust (3.5 g) was added and 20 ml conc HCl added dropwise. The solution was stirred overnight, becoming colourless. It was poured into water (200 ml), giving a white precipitate. The solid was extracted with diethyl ether (3 × 50 ml). The organic layer was washed with water, dried and evaporated. The residue was recrystallised from hexane to give pale yellow crystals of 1-phenyl-2-(4-methylphenyl)hydrazo-*ortho*-carborane (0.65 g, 89%). M.p. 148–149.5°C. Found: C, 53.0; H, 7.0; N, 8.1. $C_{15}H_{24}B_{10}N_2$ requires C, 52.8; H, 7.0; N, 8.2%. MS (EI$^+$, *m*/*z*) [M]$^+$ 336–343; 340 (100); IR ν_{max} (KBr) [cm^{-1}]: 3312s (NH), 3120, 3105 (aryl CH), 2950 (methyl CH), 2663s, 2628s, 2550s (BH), 1514s, 1262m, 814s, 689s. ^{1}H{^{11}B}

NMR ($CDCl_3$), δ: 7.69 (d, $^3J_{HH}$ 8 Hz, 2H, *ortho* C_6H_5), 7.53 (t, $^3J_{HH}$ 8 Hz, 1H, *para* C_6H_5), 7.40 (t, $^3J_{HH}$ 8 Hz, 2H, *meta* C_6H_5), 6.82 (d, $^3J_{HH}$ 8 Hz, 2H, *meta* C_6H_4Me), 6.17 (d, $^3J_{HH}$ 8 Hz, 2H, *ortho* C_6H_4Me), 5.28 (br,s, 1H, NH), 4.83 (s, 1H, N$\underline{H}$Ar), 2.83 (s, 2H, H3,6), 2.59 (s, 2H, BH), 2.41 (s, 3H, BH incl H9), 2.32 (s, 1H, H12), 2.21 (s, 3H, CH_3), 2.14 (s, 2H, H8,10); $^{11}B\{^1H\}$ NMR ($CDCl_3$), δ: –3.9 (1B, B9), –6.8 (1B, B12), –10.6 (4B), –12.6 (4B); $^{13}C\{^1H\}$ NMR ($CDCl_3$), δ: 144.9 ($\underline{C}$–CH_3), 131.8, 129.5, 128.8 (aryl CH); 131.0 (*ipso* C_6H_5), 130.5 (*para* C_6H_5), 130.1 (C–N), 112.5 ($\underline{C}$HCN), 102.3 (C1), 90.0 (C2), 20.4 (CH_3).

Preparation of carboranylhydroxylamines

The methyl nitrosocarborane (0.22 g) was dissolved in 10 ml of *p*-dioxane, 5% Pd/C (40mg) added and the solution degassed by a freeze-pump-thaw process. Hydrogen was admitted and its uptake measured using a standard hydrogenation apparatus. 25 ml of hydrogen was consumed over a period of 6 h. The solution was filtered and evaporated to leave a white solid (210 mg, 95%), M. p. 253–255°C (lit. [14] 256–258°C). Found: C, 19.4; H, 8.1; N, 6.2. $C_{15}H_{24}B_{10}N_2$ requires C, 19.1; H, 7.9; N, 7.4%. MS (EI^+, *m*/*z*) $[M]^+$ 185–192; 189 (100); IR ν_{max} (KBr) [cm^{-1}]: 3340, 3290 (NH,OH), 2914 (methyl CH), 2579s (BH), 1254s, 1116s, 1080m, 870s. $^1H\{^{11}B\}$ NMR ($CDCl_3$), δ: 5.94 (s, 1H, NH), 5.39 (s, 1H, OH), 2.46 (s, 2H, H3,6), 2.24 (s, 3H, BH), 2.22 (s, 1H, BH), 2.18 (s, 2H, BH), 2.05 (s, 2H, H8,10), 2.02 (s, 3H, CH_3); $^{11}B\{^1H\}$ NMR ($CDCl_3$), δ: –6.1 (2B, B9,12), –10.9 (4B), –11.7 (4B); $^{13}C\{^1H\}$ NMR ($CDCl_3$), δ: 94.5 (C1), 78.6 (C2), 21.6 (CH_3).

A larger-scale preparation was used for the phenyl analogue to afford 3.37 g (87%) from 3.86 g of the nitroso compound, M.p. 95–96°C, (lit. [13] 98–99°C). Found: C, 38.3; H, 6.8; N, 5.6. $C_{15}H_{24}B_{10}N_2$ requires C, 38.2; H, 7.2; N, 5.4%. MS (EI^+, *m*/*z*) $[M]^+$ 247–255; 251 (100); IR ν_{max} (KBr) [cm^{-1}]: 3532, 3463, 3280 (NH,OH), 3061 (phenyl CH), 2574s (BH), 1493m, 1446s, 1071s, 1003s, 689s. $^1H\{^{11}B\}$ NMR ($CDCl_3$), δ: 7.70 (d, 2H, *ortho* C_6H_5), 7.47 (t, 1H, *para* C_6H_5), 7.40 (t, 2H, *meta* C_6H_5), 5.69 (s, 1H, NH), 5.09 (s, 1H, OH), 2.83 (s, 2H, H3,6), 2.53 (s, 2H, BH), 2.42 (s, 3H, BH), 2.38 (s, 1H, H12), 2.17 (s, 2H, H8,10); $^{11}B\{^1H\}$ NMR ($CDCl_3$), δ:

-3.8 (1B, B9), -5.7 (1B, B12), -10.6 (4B), -12.1 (4B); $^{13}C\{^1H\}$ NMR ($CDCl_3$), δ: 131.3, 130.8 (para C), 130.0 (ipso C), 129.1, 98.4 (C1), 86.5 (C2).

Preparation of methyl-*ortho*-carboranyl amine

The compound 1-nitroso-2-methyl-*ortho*-carborane (1.50 g) was dissolved in dimethoxyethane (25 ml) and tin powder (1.50 g) was added. Concentrated HCl (25 ml) was added dropwise and the solution stirred for 15 min, after which time the blue colour had disappeared. The solution was heated to reflux for 3 h, cooled to room temperature and diluted with diethyl ether (100 ml). The solution was washed with water (3 × 50ml), dried and evaporated. The white residue was sublimed to yield 1-amino-2-methyl-*ortho*-carborane (1.10 g, 79%), M.p. 301–302°C (lit. [14] 302–303°C). Found C, 20.9; H, 9.0; N, 7.1. $C_3H_{15}B_{10}N$ requires C, 20.8; H, 8.7; N, 8.1%. MS (EI): M, 169–176 ($C_3H_{15}B_{10}N$ = 173). I.R. (cm^{-1}): 3306, 3219br (NH), 2939w (methyl CH), 2671s, 2634s, 2602s, 2580s (BH), 1491m, 1451m, 1221m, 1079s, 1026m, 1002m, 864m, 809m, 764s, 700s. $^1H\{^{11}B\}$ NMR ($CDCl_3$): 3.00 (2H, s, H4,5), 2.99 (2H, NH_2), 2.41 (2H, H7,11), 2.20 (1H, H9), 2.04 (3H, CH_3), 2.02 (2H, H3,6), 1.98 (1H, H12), 1.95 (2H, H8,10), ^{11}B NMR ($CDCl_3$): -5.5 (1B, d, B9), -9.4 (1B, d, B12), -9.8 (2B, d, B4,5), -10.6 (4B, d, B3,6,7,11), -12.5 (2B, d, B8,10). $^{13}C\{^1H\}$ NMR ($CDCl_3$): 91.1 (C1), 78.9 (C2), 21.1 (CH_3).

Crystal structure determinations

Crystals of the compounds **1**–**4** were examined on Bruker SMART (**3**) and Stoe STADI4 (**1**, **2**, **4**) diffractometers with Mo-Kα radiation (λ = 0.71073 Å; Cu-Kα with λ = 1.54184 Å for **1**) at 160 K. Crystal data and other information are given in Table 4. Standard methods and software were employed, including refinement on all F^2 values [28]; no absorption corrections were applied, and no structural disorder was found.

Table 4. Crystal data and refinement information for compounds **1**–**4**.

Compound	**1**	**2**	**3**	**4**
Formula	$C_{15}H_{22}B_{10}N_2$	$C_{15}H_{24}B_{10}N_2$	$C_9H_{20}B_{10}N_2$	$C_8H_{17}B_{10}NO\cdot\frac{1}{2}C_4H_8O_2$
M	338.5	340.5	264.4	295.38
Crystal system	monoclinic	monoclinic	monoclinic	monoclinic
Space group	*C*2/*c*	*P*2$_1$/*c*	*P*2$_1$/*n*	*P*2$_1$/*c*
a (Å)	28.695(6)	11.753(6)	8.6912(11)	12.394(1)
b (Å)	7.071(2)	7.617(4)	15.568(2)	6.714(1)
c (Å)	19.008(5)	21.899(13)	11.5680(15)	19.498(2)
β (°)	96.34(3)	104.74(6)	96.576(3)	94.30(2)
V (Å^3)	3833.2(17)	1895.9(18)	1554.9(3)	1617.9(3)
Z	8	4	4	4
Data collected	6424	4051	8134	4131
Unique data	2992	3329	3099	2846
R_{int}	0.046	0.049	0.056	0.031
Refined parameters	246	252	271	217
R (on F, F^2>2σ)	0.053	0.049	0.049	0.048
R_w (on F^2, all data)	0.154	0.137	0.126	0.134
min, max electron density (e Å^{-3})	0.25, –0.23	0.24, –0.21	0.23, –0.20	0.25, –0.21

Computational Section

AM1 [29] calculations were carried out on crystallographically determined geometries using MOPAC2002 (Version 2.40) within the CAChe 6.1 program for Windows [30]. *Ab initio* computations were carried out with the Gaussian 03 package [31]. All model geometries of HCb^{o}X and PhX with fixed torsion angles for C2–C1–N–R/X listed in Tables 4 and 5 respectively were optimized initially at the HF/6-31G* level of theory followed by the MP2/6-31G* level of theory. The geometries of PhCb^{o}X and MeCb^{o}X listed in Table 6 were optimised at the HF/6-31G* level of theory either with no symmetry constraints (and confirmed by frequency calculations to be a true minimum) or with the nitrogen atom N1 constrained to a planar configuration. These geometries were then optimised at the MP2/6-31G* level of theory.

Calculated NMR shifts at the GIAO-B3LYP/6-311G* level were obtained from these MP2-optimized geometries. Theoretical ^{11}B chemical shifts at the GIAO-B3LYP/6-311G*//MP2/6-31G* level were referenced to B_2H_6 (16.6 ppm [32]) and converted to the usual $BF_3.OEt_2$ scale: $\delta(^{11}B) = 102.83 - \sigma(^{11}B)$. The ^{13}C and ^{1}H chemical shifts were referenced to TMS: $\delta(^{13}C) = 179.81 - \sigma(^{13}C)$; $\delta(^1H) = 32.28 -$

$\sigma(^1H)$. Agreements between observed and calculated (B3LYP/6-311G*//MP2/6-31G* level) ^{11}B and ^{13}C NMR shifts generated from optimised geometries are generally very good for carboranes [33]. Agreements between observed and calculated ^1H NMR shifts in carboranes are often not as good due to a narrow ppm range (*ca* 12 ppm) and substantial solvent effects on ^1H shift measurements. [24].

Appendix A. Supplementary data

CCDC 704893–704896 contain the supplementary crystallographic data for **1**–**4** respectively. These data can be obtained free of charge via http://www.ccdc.cam.ac.uk/conts/retrieving.html or from the Cambridge Crystallographic Data Centre, 12 Union Road, Cambridge CB2 1EZ, UK; fax: (+44) 1223-336-033, or e-mail: deposit@ccdc.cam.ac.uk.

Acknowledgements

EPSRC is gratefully acknowledged for funding (MAF, RJP). We thank Durham Unversity for access to its High Performance Computing facility.

References

[1] D. A. Brown, W. Clegg, H. M. Colquhoun, J. A. Daniels, I. R. Stephenson, K. Wade, J. Chem. Soc., Chem. Commun. (1987) 889.

[2] R. Coult, M. A. Fox, W. R. Gill, K. Wade, W. Clegg, Polyhedron 11 (1992) 2717.

[3] R. Kivekäs, R. Sillanpää, F. Teixidor, C. Viñas, R. Nuñez, Acta Crystallogr., Sect. C 50 (1994) 2027; R. Kivekäs, R. Sillanpää, F. Teixidor, C. Viñas, R. Nuñez, Acta Crystallogr., Sect. *C* 51 (1995) 1864; R. Kivekäs, F. Teixidor, C. Viñas, R. Nuñez, Acta Crystallogr., Sect. C 51 (1995) 1868; J. M. Oliva, C. Viñas, J. Mol. Struct 556 (2000) 33; J. Llop, C. Viñas, J. M. Oliva, F. Teixidor, M. A. Flores, R. Kivekäs, R. Sillanpää, J. Organomet. Chem. 657 (2002) 232.

[4] L. A. Boyd, W. Clegg, R. C. B. Copley, M. G. Davidson, M. A. Fox, T. G. Hibbert, J. A. K. Howard, A. Mackinnon, R. J. Peace, K. Wade, Dalton Trans. (2004) 2786.

[5] J. M. Oliva, N. L. Allan, P. v. R. Schleyer, C. Viñas, F. Teixidor, J. Am. Chem. Soc 127 (2005) 13547.

[6] A. I. Yanovskii, Y. T. Struchkov, V. N. Kalinin, A. V. Usatov, L. I. Zakharkin, Koord. Khim. 8 (1982) 240.

[7] J. F. Valliant, O. O. Sogbein, P. Morel, P. Schaffer, K. J. Guenther, A. D. Bain, Inorg. Chem. 41 (2002) 2731.

[8] M. A. Fox, A. K. Hughes, Coord. Chem. Rev 248 (2004) 457.

[9] L. Deng, H. S. Chan, Z. Xie, J. Am. Chem. Soc. 127 (2005) 13774.

[10] M. A. Fox, J. A. H. MacBride, R. J. Peace, W. Clegg, M. R. J. Elsegood, K. Wade, Polyhedron 28 (2009) 789.

[11] M. A. Fox, J. A. H. MacBride, R. J. Peace, K. Wade, J. Chem. Soc., Dalton Trans. (1998) 401; L. A. Boyd, H. M. Colquhoun, M. G. Davidson, M. A. Fox, W. R. Gill, P. L. Herbertson, T. G. Hibbert, J. A. H. MacBride, R. J. Peace, G. P. Rivers, K. Wade, Spec. Publ. R. Soc. Chem. 201 (1997) 289.

[12] V. N. Kalinin, G. G. Zhigareva, L. I. Zakharkin, Synth. Inorg. Met.-Org. Chem. 2 (1972) 105.

[13] L. I. Zakharkin, V. N. Kalinin, Dokl. Akad. Nauk SSSR 164 (1965) 577.

[14] L. I. Zakharkin, G. G. Zhigareva, Zh. Obshch. Khim. 45 (1975) 1293.

[15] E. S. Alekseyeva, M. A. Fox, J. A. K. Howard, J. A. H. MacBride, K. Wade, Appl. Organomet. Chem. 17 (2003) 499.

[16] M. Tsuji, J. Org. Chem. 69 (2004) 4063; I. V. Glukhov, K.A. Lyssenko, A.A. Korlyukov, M.Y. Antipin, Faraday Discussions 135 (2007) 203; I. V. Glukhov, M. Y. Antipin, K. A. Lyssenko, Eur. J. Inorg. Chem. 7 (2004), 1379.

[17] Z G. Lewis, A. J. Welch, Acta Crystallogr., Sect. C 49 (1993) 705; T. D. McGrath, A. J. Welch, Acta Crystallogr., Sect. C 51 (1995) 646.

[18] R. L. Thomas, G. M. Rosair, A. J. Welch, Acta Crystallogr., Sect. C 52 (1996) 1024; I. V. Glukhov, K. A. Lyssenko, A. A. Korlyukov, M. Y. Antipin, Russ. Chem. Bull. 54 (2005) 547.

[19] D. Hnyk, J. Holub, M. Hofmann, P. v. R. Schleyer, H. E. Robertson, D. W. H. Rankin, J. Chem. Soc., Dalton Trans. (2000) 4617; D. Hnyk, D. W. H. Rankin, Dalton Trans. (2009) DOI: 10.1039/b806774k; M. A. Fox, R. Greatrex, A. Nikrahi, P. T. Brain, M. J. Picton, D. W. H. Rankin, H. E. Robertson, M. Bühl, L. Li, R. A. Beaudet, Inorg. Chem. 37 (1998) 2166.

[20] M. Buhl, P. v. R. Schleyer, J. Am. Chem. Soc. 114 (1992) 477; M. A. Fox, A. E. Goeta, A. K. Hughes, A. L. Johnson. J. Chem. Soc., Dalton Trans (2002) 2132.

[21] D. A. Fletcher, B. G. Gowenlock, K. G. Orrell, J. Chem. Soc., Perkin Trans. 2 (1998) 798.

[22] M. Barfield, P. Fagerness, J. Am. Chem. Soc. 119 (1997) 8699.

[23] S. Heřmánek, J. Plešek, V. Gregor, B. Štibr, J. Chem. Soc., Chem. Commun. (1977) 561; S. Heřmánek, D. Hnyk, Z. Havlas, J. Chem. Soc., Chem. Commun. (1989) 1859; M. Bühl, P. v. R. Schleyer, Z. Havlas, D. Hnyk, S. Heřmánek, Inorg. Chem. 30 (1991) 3107; S. Heřmánek, Chem. Rev. 92 (1992), 325; S. Heřmánek, Inorg. Chim. Acta 289 (1999) 20.

[24] E. S. Alekseyeva, A. S. Batsanov, L. A. Boyd, M. A. Fox, T. G. Hibbert, J. A. K. Howard, J. A. H. MacBride, A. Mackinnon, K. Wade, Dalton Trans. (2003) 475.

[25] M. F. Hawthorne, T. D. Andrews, P. M. Garrett, E. P. Olsen, M. Reintjes, F. N. Tebbe, L. F. Warren, P. A. Wegner, D. C. Young, Inorg. Synth. 10 (1967) 91.

[26] P. T. Brain, J. Cowie, D. J. Donohoe, D. Hnyk, D. W. H. Rankin, D. Reed, B. D. Reid, H. E. Robertson, A. J. Welch, M. Hofmann, P. v. R. Schleyer, Inorg. Chem. 35 (1996) 1701.

[27] A. Roe, Organic Reactions, vol. 5, Wiley, New York (1949).

[28] G. M. Sheldrick, Acta Crystallogr., Sect. A 64 (2008) 112.

[28] M. J. S. Dewar, E. G. Zoebisch, E. F. Healy, J. J. P. Stewart, J. Am. Chem. Soc. 107 (1985) 3902; M. J. S. Dewar, C. Jie, E. G. Zoebisch, Organometallics 7 (1988) 513.

[29] *CAChe 6.1.1 for Windows*, Fujitsu Ltd., Chiba, Japan (2003).

[30] Gaussian 03, Revision C.02, M. J. Frisch, G. W. Trucks, H. B. Schlegel, G. E. Scuseria, M. A. Robb, J. R. Cheeseman, J. A. Montgomery, Jr., T. Vreven, K. N. Kudin, J. C. Burant, J. M. Millam, S. S. Iyengar, J. Tomasi, V. Barone, B. Mennucci, M. Cossi, G. Scalmani, N. Rega, G. A. Petersson, H. Nakatsuji, M. Hada, M. Ehara, K. Toyota, R. Fukuda, J. Hasegawa, M. Ishida, T. Nakajima, Y. Honda, O. Kitao, H. Nakai, M. Klene, X. Li, J. E. Knox, H. P. Hratchian, J. B. Cross, C. Adamo, J. Jaramillo, R. Gomperts, R. E. Stratmann, O. Yazyev, A. J. Austin, R. Cammi, C. Pomelli, J. W. Ochterski, P. Y. Ayala, K. Morokuma, G. A. Voth, P. Salvador, J. J. Dannenberg, V. G. Zakrzewski, S. Dapprich, A. D. Daniels, M. C. Strain, O. Farkas, D. K. Malick, A. D. Rabuck, K. Raghavachari, J. B. Foresman, J. V. Ortiz, Q. Cui, A. G. Baboul, S. Clifford, J. Cioslowski, B. B. Stefanov, G. Liu, A. Liashenko, P. Piskorz, I. Komaromi, R. L. Martin, D. J. Fox, T. Keith, M. A. Al-Laham, C. Y. Peng, A. Nanayakkara, M. Challacombe, P. M. W. Gill, B. Johnson, W. Chen, M. W. Wong, C. Gonzalez, J. A. Pople, Gaussian, Inc., Wallingford CT (2004).

[31] T. P. Onak, H. L. Landesman, R. E. Williams, J. Phys. Chem. 63 (1959) 1533.

[32] M. A. Fox, A. K. Hughes, J. M. Malget, J. Chem. Soc., Dalton Trans. (2002**)** 3505; A. R. Turner, H. E. Robertson, K. B. Borisenko, D. W. H. Rankin, M. A. Fox, Dalton Trans. (2005) 1310; P. v. R. Schleyer, J. Gauss, M. Bühl, R. Greatrex, M.A. Fox, J. Chem. Soc. Chem. Commun. (1993) 1766; I. D. Mackie, H. E. Robertson, D. W. H. Rankin, M. A. Fox, J. M. Malget, Inorg. Chem. 43 (2004) 5387; A. S. Batsanov, M. A. Fox, A. E. Goeta, J. A. K. Howard, A. K. Hughes, J. M. Malget, *J. Chem. Soc., Dalton Trans.* (2002) 2624.